

Ouyang Ziyuan, Li Chunlai, Zou Yongliao, Zhang Hongbo, Lu Chang, Liu Jianzhong, Liu Jianjun, Zuo Wei, Su Yan, Wen Weibin, Bian Wei, Zhao Baochang, Wang Jianyu, Yang Jianfeng, Chang Jin, Wang Huanyu, Zhang Xiaohui, Wang Shijin, Wang Min, Ren Xin, Mu Lingli, Kong Deqing, Wang Xiaoqian, Wang Fang, Geng Liang, Zhang Zhoubin, Zheng Lei, Zhu Xinying, Zheng Yongchun, Li Junduo, Zou Xiaoduan, Xu Chun, Shi Shuobiao, Gao Yifei, Gao Guannan. Chang'E-1 lunar mission: an overview and primary science results. *Chinese Journal of Space Science*, 2010, 30(5): 392-403

# Chang'E-1 Lunar Mission: An Overview and Primary Science Results

Ouyang Ziyuan<sup>1,2</sup> Li Chunlai<sup>1</sup> Zou Yongliao<sup>1</sup> Zhang Hongbo<sup>1</sup>  
Lu Chang<sup>1</sup> Liu Jianzhong<sup>1</sup> Liu Jianjun<sup>1</sup> Zuo Wei<sup>1</sup> Su Yan<sup>1</sup>  
Wen Weibin<sup>1</sup> Bian Wei<sup>1</sup> Zhao Baochang<sup>3</sup> Wang Jianyu<sup>4</sup>  
Yang Jianfeng<sup>3</sup> Chang Jin<sup>5</sup> Wang Huanyu<sup>6</sup> Zhang Xiaohui<sup>7</sup>  
Wang Shijin<sup>7</sup> Wang Min<sup>1</sup> Ren Xin<sup>1</sup> Mu Lingli<sup>1</sup>  
Kong Deqing<sup>1</sup> Wang Xiaoqian<sup>1</sup> Wang Fang<sup>1</sup> Geng Liang<sup>1</sup>  
Zhang Zhoubin<sup>1</sup> Zheng Lei<sup>1</sup> Zhu Xinying<sup>1</sup> Zheng Yongchun<sup>1</sup>  
Li Junduo<sup>1</sup> Zou Xiaoduan<sup>1</sup> Xu Chun<sup>1</sup> Shi Shuobiao<sup>1</sup>  
Gao Yifei<sup>1</sup> Gao Guannan<sup>1</sup>

1(National Astronomical Observatories, Chinese Academy of Sciences, Beijing 100012)

2(Institute of Geochemistry, Chinese Academy of Sciences)

3(Xi'an Institute of Optics and Precision Mechanics, Chinese Academy of Sciences)

4(Shanghai Institute of Technical Physics, Chinese Academy of Sciences)

5(Purple Mountain Observatory, Chinese Academy of Sciences)

6(Institute of High Energy Physics, Chinese Academy of Sciences)

7(Center for Space Science and Applied Research, Chinese Academy of Sciences)

**Abstract** Chang'E-1 is the first lunar mission in China, which was successfully launched on Oct. 24th, 2007. It was guided to crash on the Moon on March 1, 2009, at 52.36°E, 1.50°S, in the north of Mare Fecunditatis. The total mission lasted 495 days, exceeding the designed life-span about four months. 1.37 Terabytes raw data was received from Chang'E-1. It was then processed into 4 Terabytes science data at different levels. A series of science results have been achieved by analyzing and applying these data, especially "global image of the Moon of China's first lunar exploration mission". Four scientific goals of Chang'E-1 have been achieved. It provides abundant materials for the research of lunar sciences and cosmochemistry. Meanwhile these results will serve for China's future lunar missions.

**Keywords** Chang'E-1, Lunar probe, Science results, China's Lunar Exploration Program, Moon

## 1 Introduction

### 1.1 China's Lunar Orbiting Project

China's Lunar Exploration Program (CLEP) was

named as Chang'E Program, and the first lunar probe was named as Chang'E-1. Chang'E is a famous Chinese mythical goddess. She ascended from the Earth and lived on the Moon as a fairy after drinking an

elixir.

The first stage of CLEP, lunar orbiting project, was subscribed by Premier Jiabao Wen, and approved by Chinese government on Jan. 23, 2004. Five systems of CLEP, which are launch vehicle system, orbiter system, Telemetry Tracking and Command (TT&C) system, launch site system, and Ground Segment for Data, Science and Application (GSDSA), were established in April, 2004.

Satellite platform, instruments and two deep space ground stations were developed and constructed in 2005–2006. Large number of tests and experiments were carried out simultaneously.

Chang'E-1 was launched on Oct. 24, 2007. It means that China has taken a first step in the field of lunar exploration. The implementation of CLEP opened the window of China's deep space exploration. It marked a new milestone in China's aerospace industry after Earth satellites and manned spaceflight.

## 1.2 Operations and Maneuver of Chang'E-1 Mission

Chang'E-1 blasted off on a Long March 3A carrier rocket at 10:05 GMT on Oct. 24, 2007, from the No. 3 launching tower at the Xichang Satellite Launch Center in Southwest China.

After launch, Chang'E-1 lunar probe experienced active phase orbit, phasing orbit, cislunar transfer orbit and circumlunar orbit of trajectory (Figure 1). It took 13 days 14 hours 19 minutes in Chang'E-1's journey from the Earth to the Moon. The flight distance is 2 090 000 km.

Chang'E-1 CCD camera was firstly powered on Nov. 20, 2007. The science data from Chang'E-1 were received by Beijing and Kunming ground station simultaneously. The first image from Chang'E-1



Figure 1 Operations and maneuver of Chang'E-1 probe.

was released on Dec. 26, 2007. One year later, the first vision of global image of the Moon was released on Dec. 12, 2008.

Chang'E-1 was guided to crash on the surface of the Moon and ended its life at 08:13:10 UTC, on March 1st, 2009. Impact point was located at 52.36°E, 1.50°S, in the north of Mare Fecunditatis.

## 2 Science Goals and Instruments

### 2.1 Science Goals

There are four scientific goals of Chang'E-1 lunar probe<sup>[1–3]</sup>.

The first goal of Chang'E-1 is to obtain images of the Moon and to map global 3D stereo images of the Moon<sup>[4–8]</sup>. 3D stereo images are basic materials to study the surface features of the Moon. Using these data, the topography, geologic units of the lunar surface and tectonic outline-graphs of the Moon could be outlined<sup>[9–10]</sup>. The information can also provide reference for site selection of China's future soft-landing on the Moon.

The second goal is to retrieve the abundance of some key elements on lunar surface. One set of Sagnac-based interferometer spectrometer, one set of  $\gamma$ -ray spectrometer and one set of X-ray spectrometer were developed and served for this purpose. These results could be used to obtain the distribution of major rocks and minerals, and to evaluate the amount of important resource of the Moon<sup>[11–14]</sup>.

The third goal is to measure the microwave brightness temperature ( $T_B$ ) of the Moon. Combining with information about lunar surface properties<sup>[15–17]</sup>, brightness temperature data of the Moon could be used to derive thickness of lunar regolith layers. Furthermore, the resource amount of helium-3 can be estimated. A multi-channel microwave radiometer was developed and served for this purpose.

The fourth goal is to detect the space environment near the Moon, including temporal and spatial variation on the composition, flux and energy spectrum of solar wind<sup>[18–19]</sup>. These data could be used to study the influence effect of solar activity on the Earth and the Moon. One set of high-energy particle detector and two sets of solar wind ion detectors were developed and served for this purpose.

## 2.2 Scientific Instruments

To achieve the above four science goals of the mission, eight sets of scientific instruments were chosen as payloads on Chang'E-1 lunar orbiter, including CCD stereo camera (CCD), Sagnac-based Interferometer Spectrometer (IIM), Laser Altimeter (LAM), Microwave Radiometer (MRM),  $\gamma$ -Ray Spectrometer (GRS), X-Ray Spectrometer (XRS), High-energy Particle Detector (HPD), and Solar Wind Ion Detectors (SWID). The science goals and corresponding scientific instruments are introduced as follows<sup>[1]</sup>.

### Science goal:

#### To achieve three-dimensional stereoscopic image of the Moon

**Instrument** Three-line array CCD stereo camera.

**Principles** The Chang'E-1 CCD stereo camera was designed to get 3 planar images for the same object from three different view angles (forward, nadir and backward), which made it possible to get DEM data and orthophoto image data of the global lunar surface.

#### Technical indexes

Spectral range: 500–750 nm.

Optical channel: 1.

Swath width: 60 km.

Base-height ratio:  $\geq 0.6$ .

Imaging region: 70°N–70°S.

Pixel spatial resolution (sub-satellite point): 120 m.

**Instrument** Laser altimeter.

**Principles** Laser pulses were transmitted from Chang'E-1 laser altimeter to the lunar surface. The range from the orbiter to lunar surface was determined by measuring the time delay between transmission of a laser pulse and detection of the back scattered signal from the lunar surface. The altitude of the lunar surface could be calculated from the distance between the spacecraft and the nadir point of the lunar surface.

#### Technical indexes

Range of distance measurement: 200 km  $\pm$  25 km.

Footprint on the lunar surface:  $\leq \Phi 200$  m.

Laser wavelength: 1064 nm.

Laser energy: 150 mJ.

Laser pulse width: 5–7 ns.

Repetition rate of laser pulse: 1 Hz.

Aperture of reception telescope: 140 mm.

Focal length of reception telescope: 538 mm.

Range resolution: 1 m.

Ranging error: 5 m.

### Science goal:

#### To derive the chemical and mineral composition of the lunar surface

**Instrument** Sagnac-based interferometer spectrometer.

**Principles** The Sagnac-based interferometer spectrometer was developed to obtain the multi-spectral image of the lunar surface. Then the composition of lunar surface materials could be retrieved.

#### Technical indexes

Swath width: 25.6 km.

Pixel spatial resolution (sub-satellite point): 200 m.

Imaging region: 70°N–70°S.

Spectral range: 480–960 nm.

Optical channel: 32.

Pixel numbers: 256  $\times$  256

(after 2  $\times$  2 pixels combination).

$S/N$ :  $\geq 100$ .

**Instrument**  $\gamma$ -ray spectrometer.

**Principles** In order to retrieve abundances of major elements on the lunar surface, the  $\gamma$ -ray spectrometer was developed to measure the  $\gamma$ -ray photons transmitted from the lunar surface materials. Using GPS data, the abundance and distribution of some major elements could be derived.

#### Technical indexes

CsI crystal of main detector:  $\phi 118 \times 78$  (mm).

Anticoincidence crystal: 30 mm bottom-thickness, 30 mm side thickness.

Energy resolution of  $\gamma$ -ray spectrometer: 9%<sup>137</sup>Cs at 662 keV.

Energy range: 300–9000 keV.

Number of energy bands: 512 or 1024.

**Instruments** X-ray spectrometer.

**Principles** The X-ray spectrometer was developed to measure the energy spectrum of fluorescence X-rays transmitted from the lunar surface, which is excited by cosmic ray.

#### Technical indexes

Effective area of the detector: 17 cm<sup>2</sup>.

Energy range: 1–60 keV.

Resolution:  $\leq 10\%$  at 59.5 keV (Hard X-ray),  
 $\leq 600$  eV at 5.95 keV (soft X-ray).  
 Intrinsic resolution on the lunar surface:  
 170 km  $\times$  170 km (for orbit altitude 200 km).  
 Energy range of solar monitor: 1–10 keV.  
 Energy resolution of solar monitor:  
 $\leq 600$  eV at 5.95 keV.

**Science goal:**

**To retrieve physical properties and thickness of lunar regolith layers**

**Instrument** Microwave radiometer.

**Principles** The microwave radiometer was developed to measure the microwave brightness temperature of the lunar surface. The physical properties and thickness of lunar regolith layer could be derived from. Furthermore, we can estimate quantity and distribution of helium-3 resource on the Moon.

**Technical indexes**

Frequency channels: 3.0 ( $\pm 1\%$ ) GHz,  
 7.8 ( $\pm 1\%$ ) GHz, 19.35 ( $\pm 1\%$ ) GHz,  
 and 37 ( $\pm 1\%$ ) GHz.

Integration time: 200 ( $\pm 15\%$ ) ms.

Brightness temperature sensitivity:  $\leq 0.5$  K.

Linearity:  $\geq 0.99$ .

**Science goal:**

**To probe the space environment near the Moon**

**Instrument** High-energy particle detector.

**Principles** The high-energy particle detector was developed to measure the energy spectrum and flux of heavy ions and protons near the Moon.

**Technical indexes**

Electrons: two energy level

( $E_1: \geq 0.095$  MeV.  $E_2: \geq 2.2$  MeV).

Protons: six energy level

( $P_1: 4\text{--}8$  MeV.  $P_2: 8\text{--}15$  MeV.

$P_3: 15\text{--}32$  MeV.  $P_4: 32\text{--}70$  MeV.

$P_5: 70\text{--}160$  MeV.  $P_6: 160\text{--}400$  MeV).

**Instrument** Solar wind ion detectors.

**Principles** The solar wind ion detectors were developed to measure the composition and distribution of low-energy solar wind ions near the Moon. The characteristic parameters of quiet solar wind and high speed solar wind could be retrieved.

**Technical indexes**

Energy range: 0.05–20 keV.

Number of energy bands: 48.

Velocity of solar wind: 150–2000 km/s.

Instantaneous field of view:  $6.7^\circ \times 180^\circ$ .

Acceptance angle:  $6.7^\circ \times 15^\circ$ .

### 3 Science Data of Chang'E-1 Mission

During its 495 days' life-span, eight sets of scientific instruments aboard Chang'E-1 probe transmitted 1400 Gigabytes (GB) raw data to the ground station. GSDSA has processed and produced about 4000 GB science data at different levels (Table 1). The definitions of data at different level data are shown in Table 2. The level 2 and level 3 science data have been released to Chinese science communities since 2008.

### 4 Primary Science Results of Chang'E-1 Mission

Primary science results, which were derived from Chang'E-1 data are concluded as follows.

**Table 1 Amount of science data of Chang'E-1 at various levels (Megabytes, MB).**

data amount/MB	CCD	IIM	LAM	GRS	XRS	MRM	HPD	SWID	Total
Raw data									1 389 641
0 level	433 730	692 464	5 766	72 788	45 792	30 272	1 524	97 794	1 380 130
1 level	30 696	201 385	9 845	22 188	19 524	17 206	3 459	30 734	335 037
2 level	78 029	560 332	926	37 318	56 005	1 334	6 335	79 370	819 649
3 level	3 500		2.39	42			108	7 623	11 273
Total	545 955	1 454 181	16 537	132 336	121 321	48 812	11 426	215 521	3 935 730
Data characteristics	Global coverage	cover 84% area of the surface	9 120 000 points ranging	88 days' integrated data	74 days' integrated data	8 times global coverage	120 day's integrated data		

**Table 2** Definition of science data of Chang'E-1 mission.

levels	data description
raw data	Raw data was baseband data received from data transmission receiver in the ground stations
Level 0A	Level 0A data was produced after the procedure of frame synchronization, descrambling and decompression. The UTC time was added
Level 0B	Level 0B data was produced after sequencing, removing duplication and optimized stitching for Level 0A from two ground stations
Level 1	Level 1 data was produced after format reorganization and physical quantity conversion of level 0B data, and description about the data was added
Level 2	Level 2 data was produced after radiometric calibration, geometric correction and photometric correction of Level 1 data. Level 2 data could be produced farther into level 2A, 2B and 2C different sublevel
Level 3	Level 3 data was produced after deep processing based on the Level 2 data

#### 4.1 Three-Dimensional Stereoscopic Image of the Moon

From Nov. 20, 2007 to Jul. 1, 2008, the CCD camera successfully mapped the whole surface of the Moon, including the polar areas, where the solar illumination was quite weak. Generally, orbital image data are distinctly affected by altitude, solar elevation angle, incidence angle, view angle, exposure time and so on. Data preprocessing is to eliminate the above factor in order to get uniform data in the same situation. The data preprocessing for lunar images includes radiometric calibration, geometric correction, and photometric correction. After above preprocessings, we get only the single track of radiance image data. Procedure of map-making, such as projecting, geometric positioning and mosaicking, cartographic editing, is just to warp all tracks of images and create a global map. 589 tracks of image data, most of which have vertical view angles, have been used to produce a global map of the Moon.

(1) The first lunar image from Chang'E-1 is a combination product of 19 tracks image data received since Nov. 20–21, 2007. It was released on Nov. 26, 2007 (Figure 2).

(2) Three two-dimensional images, obtained by Chang'E-1 lunar probe, were processed into a three-dimensional image at the same time<sup>[20]</sup> and released on Nov. 26, 2007 (Figure 3).

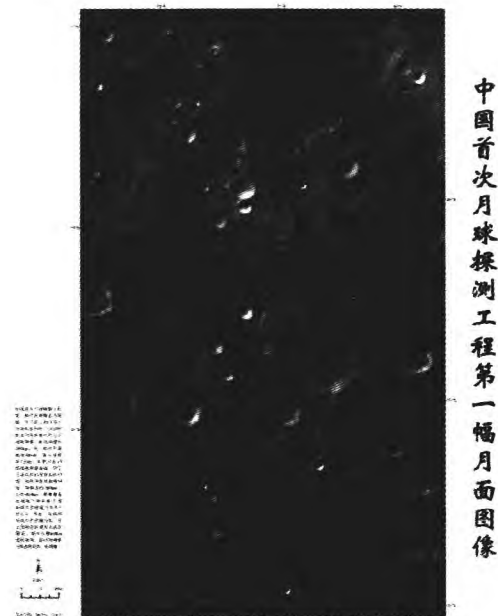


Figure 2 First lunar image obtained by Chang'E-1 lunar mission.



area in Figure 2

Figure 3 Three-dimensional image obtained by Chang'E-1 lunar mission.

(3) Using image data, plane and 3D topography maps of some important lunar geologic units image, *e.g.*, marcs, mounts, lacus, sinus, vallis, rimas, Crater Tycho and craters named after Chinese names Chang-Ngo, Chang Heng, Wan-Hoo, and Kuo Shou Ching, were produced.

(4) Laser Altimeter (LAM) achieved 9.16 million points ranging data of the lunar surface. These ranging data, with accuracy of 100 m and cross-track spacing of 80 km, depict the global DEM shape of the Moon in a center-of-mass frame. Pointing accuracy is a few tenths of a degree, leading to positioning er-

ror of several kilometers. Figure 4 are global digital elevation model of the Moon derived from Chang'E-1 LAM data.

(5) Since Nov. 20, 2007 to July 1, 2008, the CCD camera successfully mapped the whole surface of the Moon, including the polar areas, where the solar illumination was quietly weak. 589 tracks of image data, most of which have vertical view angles, have been used to make a global image of the Moon (Figure 5)<sup>[21]</sup>. The global image of the Moon was released on Nov. 12, 2008.

(6) Using 500 m spatial resolution DEM derived from CCD image, we have produced 3D topography of some important lunar geologic units. The following is a 3D map of a crater with typical central peak (Figure 6)<sup>[20]</sup>.

(7) We are still producing and developing global 3D maps of the Moon. Diameter and distribution density of craters, distribution of linear and circular structures are analyzing. These maps will be released in the near future.

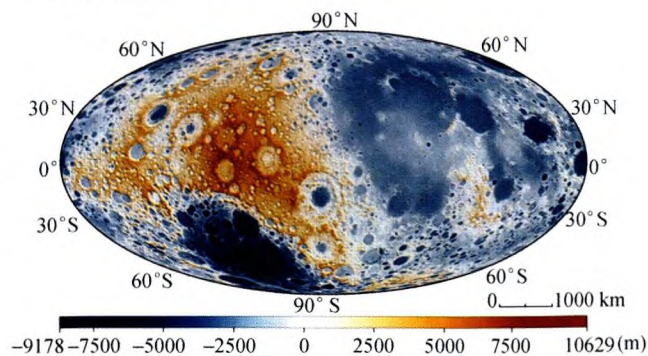


Figure 4 Global DEM of the Moon derived from Chang'E-1 LAM data.

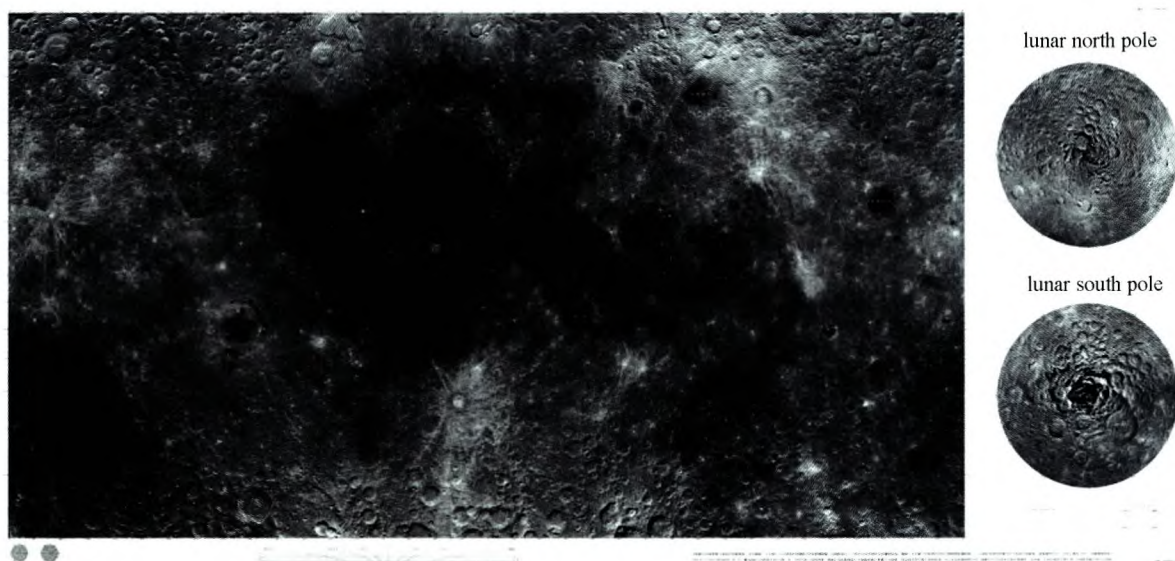


Figure 5 Global image map of the Moon of CLEP.

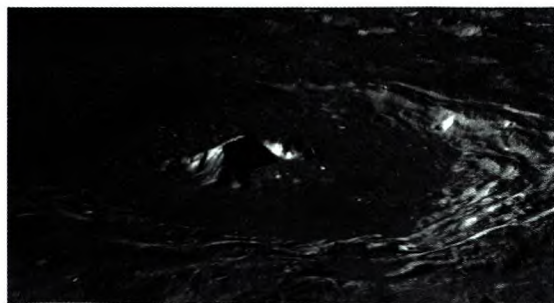


Figure 6 3D map of a crater with typical central peak (spatial resolution is 500 m).

#### 4.2 Chemical and Mineral Composition of Lunar Surface

The distribution of element abundance and rock types are important for understanding the formation and evolution of the Moon. Three sets of instruments on Chang'E-1, sagnac-based interferometer spectrometer,  $\gamma$ -ray spectrometer and X-ray spectrometer were selected to derive the distribution of chemical compositions and minerals on the lunar surface. Chang'E-1 IIM images, reflectance properties of Moon, were used to derive the chemical and mineral composition of

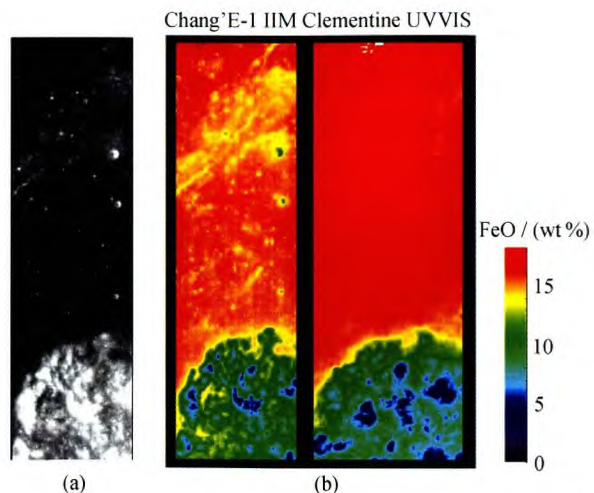


Figure 7 FeO abundance of the lunar surface in the Mare Crisium. (a) Image data was sampled at 757 nm of the 2185 orbit of Chang'E-1 IIM; (b) Iron abundance of the lunar surface in the Mare Crisium, left color map was derived from Chang'E-1 IIM data, and right color map was derived from Clementine UVVIS data.

lunar surface (Figure 7).  $\gamma$ -ray spectrometer and X-ray spectrometer data were used to derive the abundance of some key elements. These instruments were calibrated by our lunar highland<sup>[21]</sup> and mare<sup>[22]</sup> soil simulants.

Using inversion model of elemental abundances proposed by Lawrence (2000), the global abundance maps of radioactive elements U, K and Th had been acquired (Figure 8 and Figure 9).

Throughout normal solar conditions, Chang'E-1 XRS was able to detect abundance of Mg, Al and Si of the lunar surface materials. During solar flare events, it might detect other elements such as Ca, Ti and Fe. It is known that the X-ray emission from the lunar surface is excited by solar X-ray photons. Unfortunately, 2008 was the solar minimum year in 23-years' solar cycle, which means that the solar X-ray flux was the lowest. As a result, the fluorescent X-rays excited by the solar X-rays were so few. Thus the elemental abundance distribution could hardly be achieved. The onboard solar monitor recorded solar X-ray bursts since Dec. 31, 2007 to Jan. 2, 2008, these data could be used to detect abundance of Mg, Al and Si in the area of 3 000 000 km<sup>2</sup> of the Moon.

Chang'E-1 IIM completed 84% coverage of the lunar surface between 70°S and 70°N. A series of models have been developed to evaluate iron abundance from Clementine UVVIS images. We have developed preliminary algorithms to map FeO and TiO<sub>2</sub> abundances from Chang'E-1 IIM images. Combined with abundance of some key elements derived from GRS and XRS data, the distribution of KREEP rocks, basalt and plagioclase can be outlined.

### 4.3 Thermal Properties and Thickness of Lunar Regolith Layers

A set of four channel Microwave Radiometer (MRM) was boarded on Chang'E-1, which worked at 3.0 GHz, 7.8 GHz, 19.35 GHz and 37 GHz. Up to now, Chang'E-1 MRM is the first attempt of passive microwave

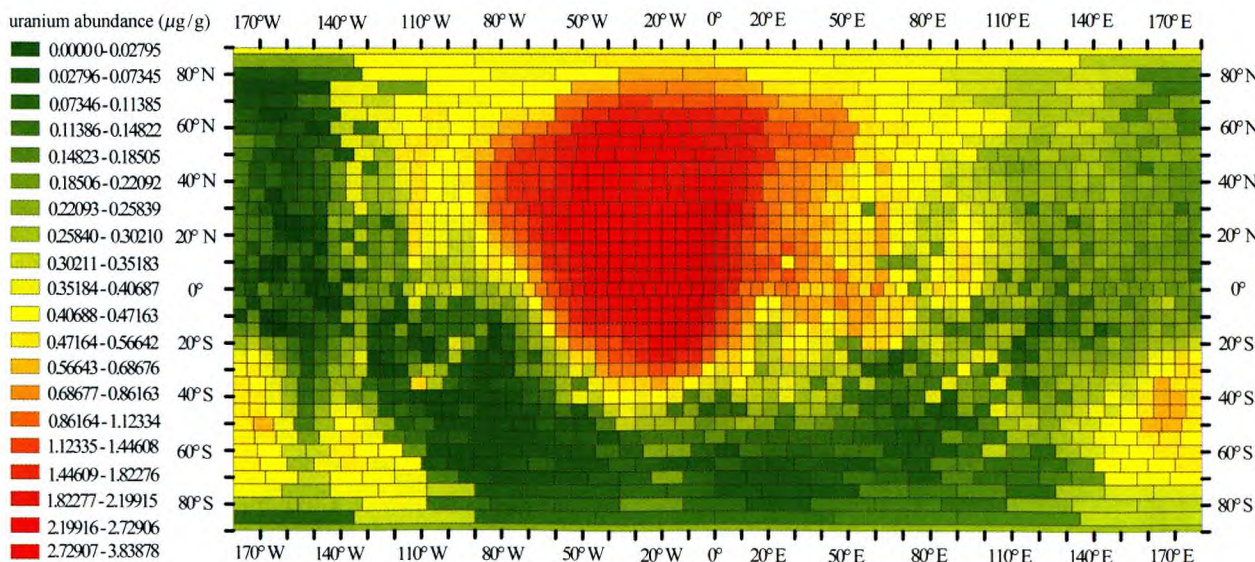


Figure 8 Global map of uranium abundance (a pixel is 5° × 5° for longitude and latitude).

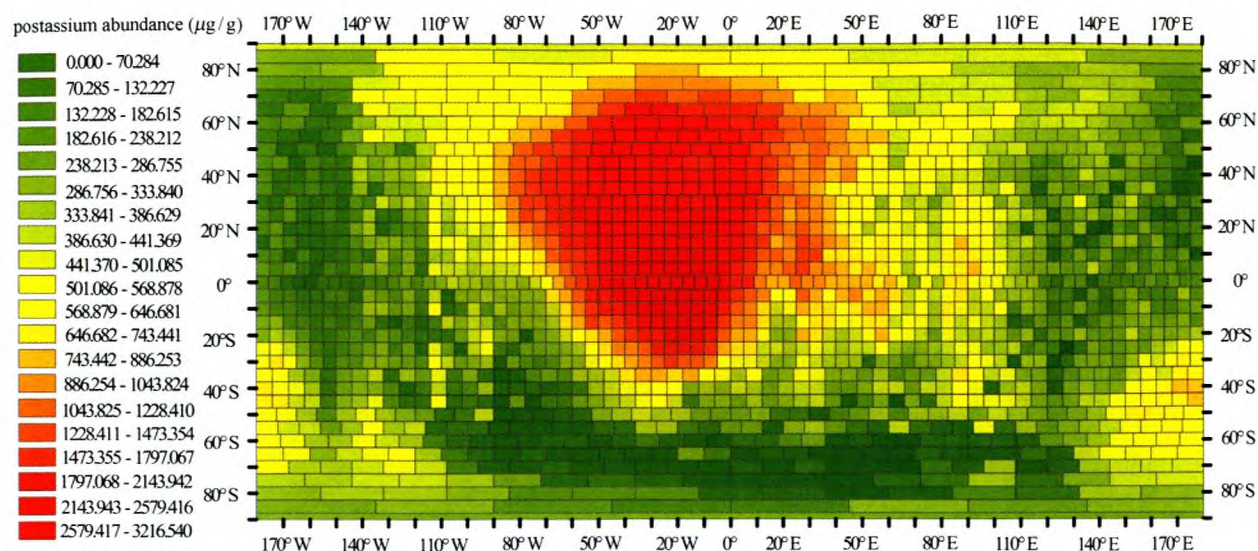


Figure 9 Global map of Potassium abundance (a pixel is  $5^\circ \times 5^\circ$  for longitude and latitude).

remote sensor in all lunar orbiters. It had completed eight times coverage to measure the microwave radiation of the Moon. The spatial resolution, temperature sensitivity, and coverage of Chang'E-1's brightness temperature ( $T_B$ ) data sets are much better than any other ground-based observation by radio observatories<sup>[23–26]</sup>. Since the wavelength of microwave is much longer than visible band, microwave radiation can penetrate the loose lunar surface materials from about a few centimeters to several tens of meters. Thus, thermal properties of regolith layers could be retrieved from brightness temperature data sets<sup>[27]</sup>.

Brightness temperature ( $T_B$ ) of the Moon was measured and calibrated by orbital two-point calibration. The contribution of radio sources for brightness temperature, which could contribute to the cold sky calibrating antenna of Chang'E-1 MRM, were eliminated. The data batch processing method was established, errors were estimated. We also have constructed microwave radiation transfer model of the Moon.

The preliminary algorithm, which was used to derive the thermal properties and thickness of regolith layer from brightness temperature data, have been proposed. The physical model of the lunar regolith could be idealized and simplified as three layer model, that is dust layer, regolith layer and bedrock layer. The correlation between brightness tempera-

ture and thickness of regolith layer, could be resolved by brightness temperature simulation for the layered mediums.

In the future, other factors that would contribute to brightness temperature of the Moon, such as surface roughness, volume scattering effects produced by rock blocks in the regolith, layered structure of lunar regolith, should be considered. Microwave radiation transfer model of the Moon will be improved and refined.

Daytime and nighttime brightness temperature of the Moon at frequency of 3.0 GHz, 7.8 GHz, 19.35 GHz, 37.0 GHz were mapped (Figure 10–11). The maps show that brightness temperature in higher latitude zone is lower than that in low latitude. Large craters, boundaries between mare and highland, basins can be identified clearly from the map. It suggests that brightness temperature is majorly controlled by lunar topography. Hot regions are presented in dark mare, where contains more abundant titanium-containing mineral ilmenite in the mare. Ilmenite is highly lossy material, which can absorb more microwave radiations than anorthite in the highland.

#### 4.4 Space Environment Near the Moon

One set of High energy Particle Detector (HPD) and two sets of Solar Wind Ion Detectors (SWIDs) are onboard to detect the space environment in the lunar orbit. During its operation, Chang'E-1 passed the



interplanetary space, the lunar wake, Magnetosheath (MS) and Magnetotail (MT) of the Earth. Counts from HPD were rare in the interplanetary space, while it observed electrons of 0.1 MeV in MS and MT (Figure 12).

Chang'E-1's solar wind ions detectors revealed

more abundant informations than HPD (Figure 13). SWID's data revealed several characteristics of geospace plasma. In the interplanetary space, solar wind plasma shows typical characteristics of large density, low temperature and few disturbances. Plasma temperature and disturbance were enhanced when

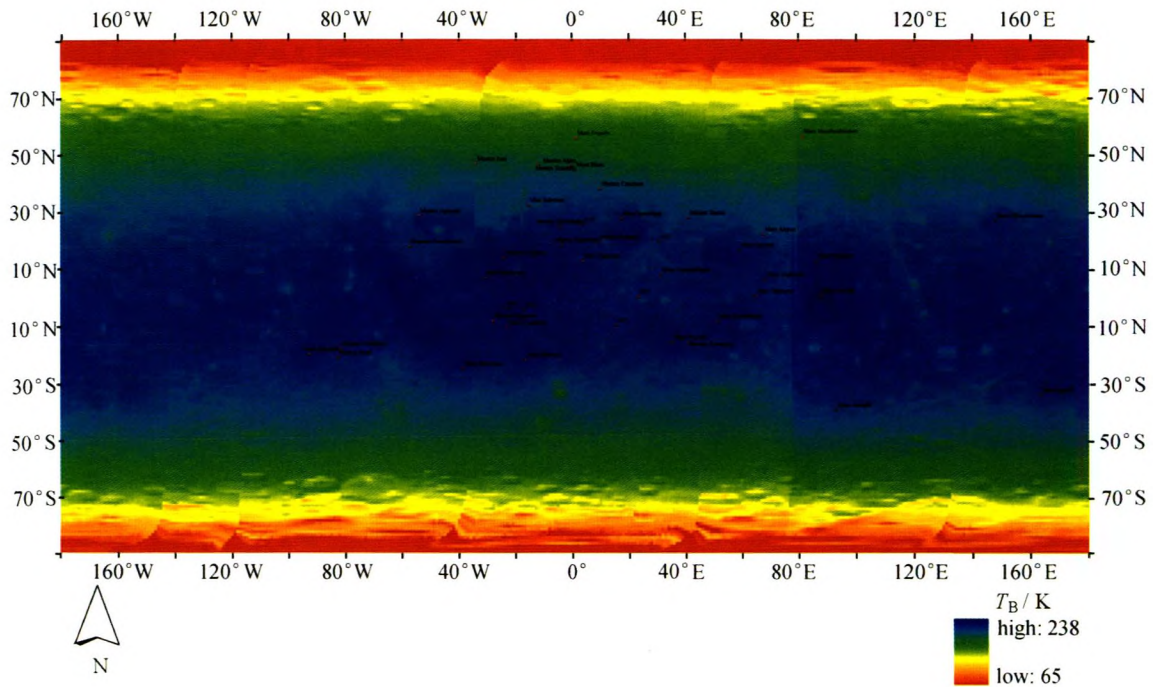


Figure 10 Lunar nighttime brightness temperature of the Moon at frequency of 37.0 GHz.

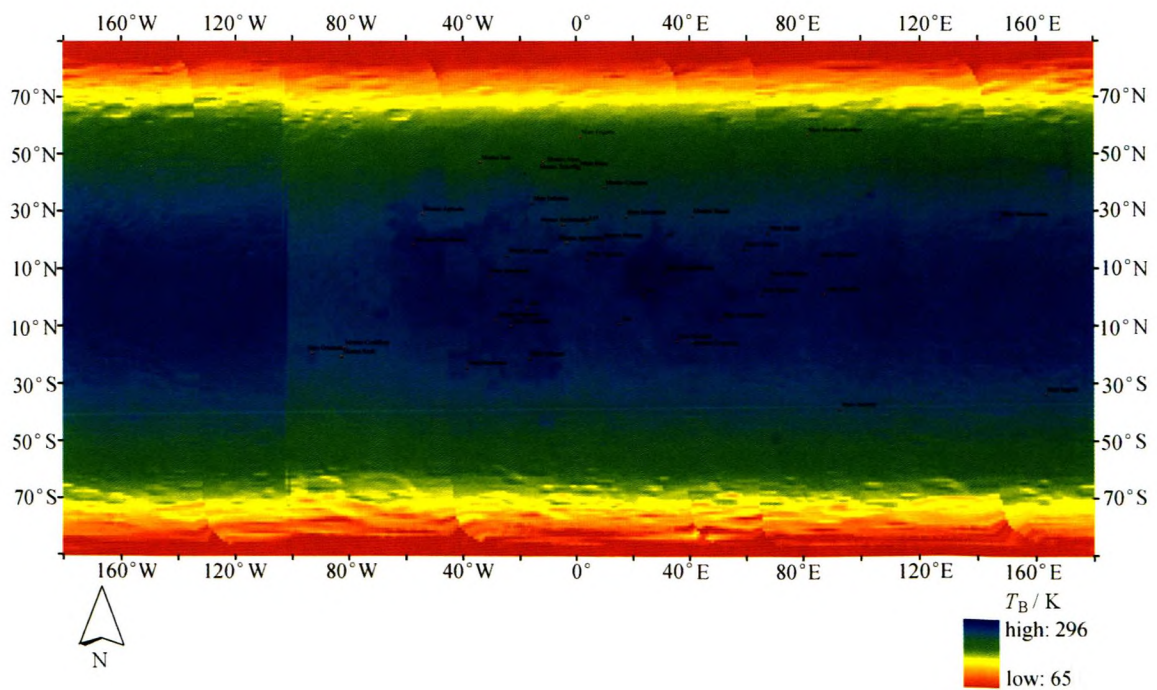


Figure 11 Lunar daytime brightness temperature of the Moon at frequency of 37.0 GHz.

Chang'E-1 passed through the magnetic sheath of Earth's geomagnetic field. While in the magnetotail, the density of solar wind ions is very low. Meanwhile, the proton temperature is high.

SWIDs also observed newly discovered reflected solar wind protons<sup>[27]</sup>. The acceleration of reflected protons in dayside of lunar surface and the polar terminator region revealed some new details of the kinetic nature of the interaction between solar wind and the Moon.

**4.5 Controlled Impact on the Moon**

The velocity of Chang'E-1 was reduced to 1.627 km/s after operations and maneuvers on Mar. 1, 2009. The CCD camera was powered on from 59 km altitude above the lunar surface when Chang'E-1 was guided and aimed at the impact point within Mare Fe-cunditatis. At 16:13:10 LT, Mar. 1, 2009, Chang'E-1

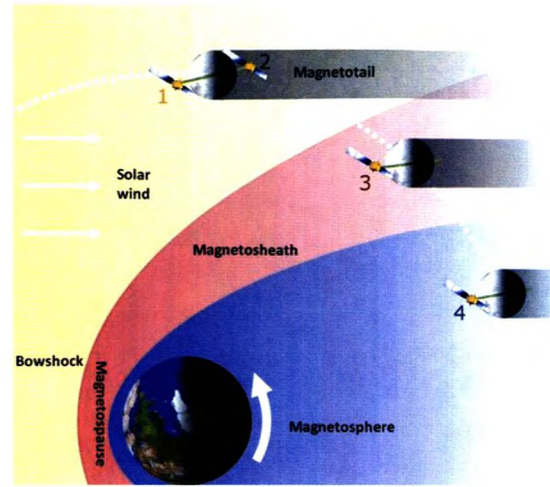


Figure 12 Four space regions where space environment data have been obtained by Chang'E-1 lunar probe.

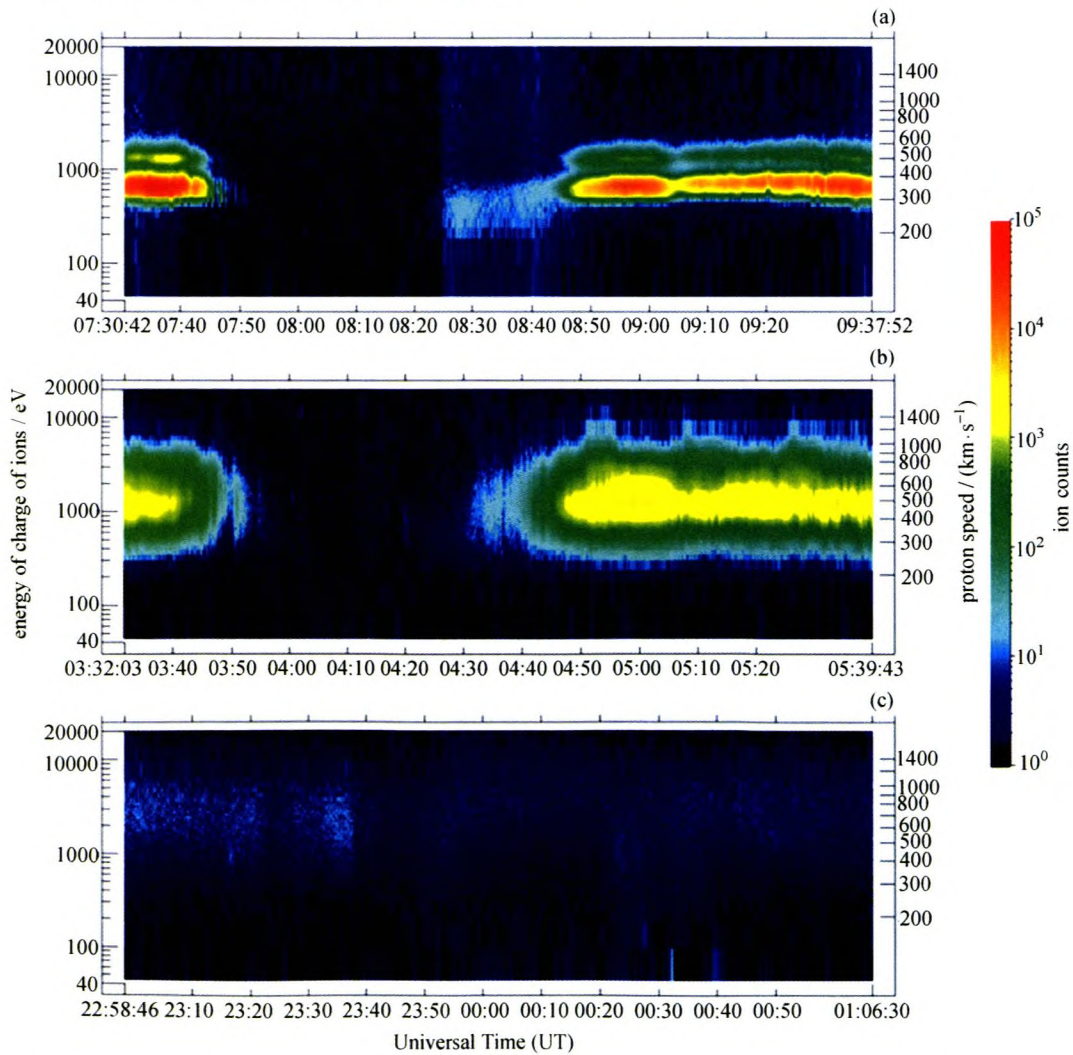


Figure 13 Energy spectrum of solar wind ions. (a) in the interplanetary space (orbit 600), (b) in the magnetic sheath of the Earth (orbit 236), (c) in the magnetotail (orbit 539).

impacted on the Moon at the site of 52.36°E, 1.50°S. The CCD camera has mapped the 1469 km images of the Moon surface before the crash (Figure 14).

### 5 Conclusion and Discussion

Through the success of Chinese first lunar exploration project, a number of key technologies have been broken through, such as the processing methods of CCD image, procedure of global image mapping, automatic DEM generation from Chang'E-1's CCD images, processing method of LAM ranging data, processing method of combination of CCD image and LAM data. We also acquired some innovative science results in the research and application of Chang'E-1 data. These results have been and will be presented and published in the journals, conferences, and patents.

The global image map of the Moon has been ac-

quired from Chang'E-1 CCD image. This image map covers the whole Moon at uniform spatial resolution of 120 m. The Chinese global image map of the Moon provides a new, highly uniform and precise data for lunar topographic demonstration and research. Because the CCD data is based on the three-line CCD stereo camera, it is possible to map 3D Moon at a very high resolution. After extracting the DEM data based on the three line array data by the photogrammetry method, the 1:2 500 000 global digital relief map with contour interval  $\leq 500$  m and 100% coverage has been released. Global DEM of the Moon, which are derived from 9.16 million points ranging data of Chang'E-1 laser altimeter, has been produced. In the geologic and geographic research, and selection of landing sites for the lander and rover, the new images and 3D maps will play important roles.

As the first attempt of passive microwave remote sensor in all lunar orbiters, Chang'E-1 MRM has co-

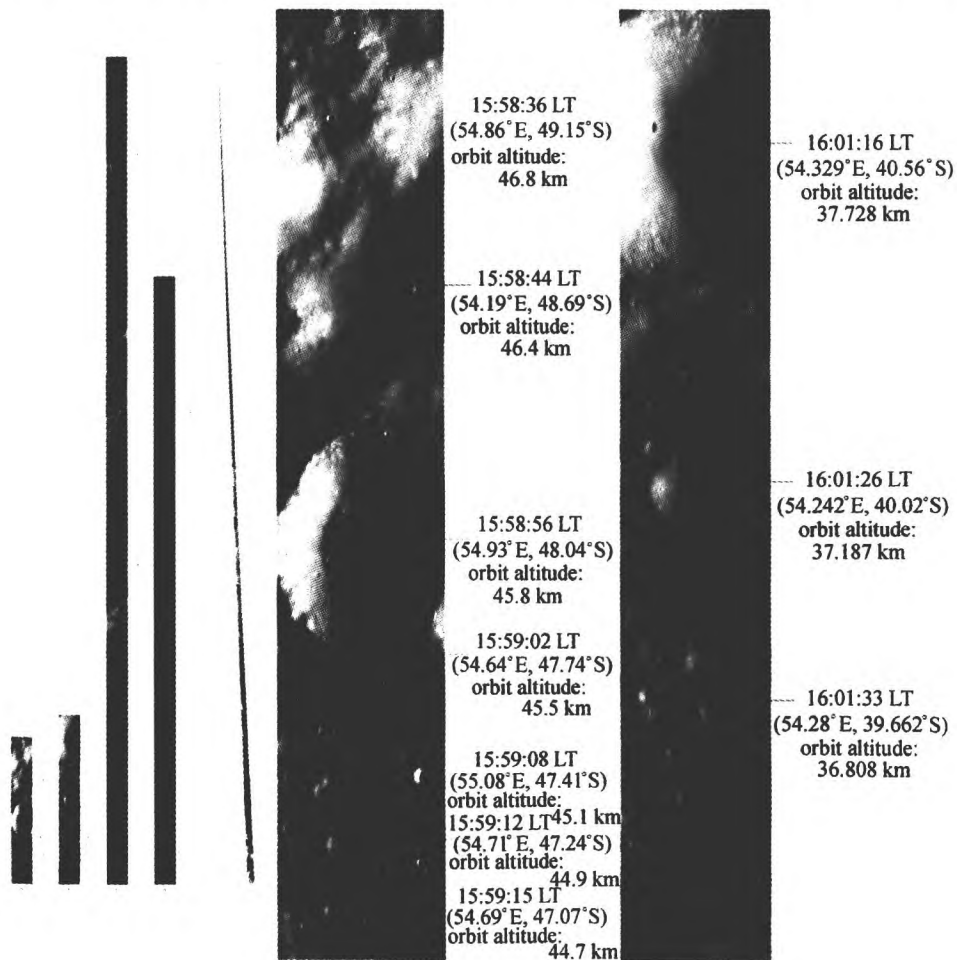


Figure 14 Mosaic of last images from Chang'E-1 before its controlled impact.

mpleted eight times coverage to measure the microwave radiation of the Moon. The spatial resolution, temperature sensitivity, and coverage of Chang'E-1's brightness temperature ( $T_B$ ) data sets are much better than any other ground-based observation by radio observatories. The thickness of lunar regolith at some typical regions has also been derived from brightness temperature data. Thermal properties of regolith layers could be retrieved in the future<sup>[28]</sup>. Chang'E-1's brightness temperature data sets suggest that brightness temperature of the Moon is controlled obviously by the topography and composition of lunar surface materials.

A large amount of meaningful data by HPD and SWIDs that are meaningful. From these data we can learn the space environment characteristics in different space areas around the Moon. As a weakly magnetized airless body, the Moon interacts with solar wind directly, which produces some unique features. Combing the recent Japanese, Indian and Chinese lunar missions, the plasma environment close (100–200 km altitude) to the Moon was firstly extensively detected.

Chang'E-1's GRS, IIM and XRS have achieved the abundance of some key elements and distribution of major minerals of the Moon. Using these results, we can outline the distribution of KREEP rocks, mare basalt and highland plagioclase. Fine tectonic map will be presented based on Chang'E-1 data in the future.

The success of Chang'E-1 is the first step of Chinese deep space exploration. Large amount of science data were produced from eight sets of instruments. We also have made beneficial attempts in data processing and retrieving algorithms. Subsequent science results have been submitted to relative journals and conferences, and will be published in the near future.

**Acknowledgements** China's lunar orbiting project is a joint accomplishment under cooperation of China National Space Administration, General Armament Department, Chinese Academy of Sciences, China Aerospace Science and Technology Corporation. In the receiving, processing and application research of Chang'E-1 data, we get help and support from many universities and institutions. The authors would like to thank all engineers and scientists who contribute to the project.

## References

- [1] Ouyang Z Y, Jiang J S, Li C L, et al. Preliminary scientific results of Chang'E-1 lunar orbiter [J]. *Chin. J. Space Sci.*, 2008, **28**(5):9-17
- [2] Ouyang Z Y. Introduction to Lunar Science [M]. Beijing: China Astronautic Publishing House, 2005. 362
- [3] Heiken G H, Vaniman D T, Frend B M. Lunar Sourcebook – A User's Guide to the Moon [M]. Cambridge: Cambridge University Press, 1991. 735
- [4] Haruyama J, Ohtake M, Matsunaga T, et al. Long-lived volcanism on the lunar farside revealed by SELENE terrain camera [J]. *Science*, 2009, **323**(5916):905-908
- [5] Lucey P G, Blewett D T, Jolliff B L. Lunar iron and titanium abundance algorithms based on final processing of Clementine ultraviolet-visible images [J]. *J Geophys. Res.*, 2000, **105**(E8):20 297-20 305
- [6] Pieters C M, Goswami J N, Clark R N, et al. Character and spatial distribution of OH/H<sub>2</sub>O on the surface of the moon seen by M3 on Chandrayaan-1 [J]. *Science*, 2009, **326**(5952):568-572
- [7] Ono T, Kumamoto A, Nakagawa H, et al. Lunar radar sounder observations of subsurface layers under the near-side maria of the Moon [J]. *Science*, 2009, **323**(5916):909-912
- [8] Namiki N, Iwata T, Matsumoto K, et al. Farside gravity field of the moon from four-way doppler measurements of SELENE (Kaguya) [J]. *Science*, 2009, **323**(5916):900-905
- [9] Araki H, Tazawa S, Noda H, et al. Lunar global shape and polar topography derived from Kaguya-LALT laser altimetry [J]. *Science*, 2009, **323**(5916):897-900
- [10] Institute of Geochemistry, Chinese Academy of Sciences. Research Progress in Lunar Geology [M]. Beijing: Science Press, 1977
- [11] Alha L, Huovelin J, Nygard K, et al. Ground calibration of the Chandrayaan-1 X-ray Solar Monitor (XSM) [J]. *Nucl. Instrum. Methods*, 2009, **607**(3):544-553
- [12] Crawford I A, Joy K H, Kellett B J, et al. The scientific rationale for the C1XS X-ray spectrometer on India's Chandrayaan-1 mission to the Moon [J]. *Planet Space Sci.*, 2009, **57**(7):725-734
- [13] Grande M, Maddison B J, Howe C J, et al. The C1XS X-ray spectrometer on Chandrayaan-1 [J]. *Planet Space Sci.*, 2009, **57**(7):717-724
- [14] Ogawa K, Okada T, Shira K, et al. Numerical estimation of lunar X-ray emission for X-ray spectrometer onboard SELENE [J]. *Earth Planets Space*, 2008, **60**(4):283-292
- [15] Haruyama J, Ohtake M, Matsunaga T, et al. Lack of exposed ice inside lunar south pole Shackleton crater [J]. *Science*, 2008, **322**(5903):938-939
- [16] Ohtake M, Matsunaga T, Haruyama J, et al. The global distribution of pure anorthosite on the Moon [J]. *Nature*, 2009, **461**:236-240
- [17] Zheng Y C, Wang S J, Ouyang Z Y. Dielectric properties of lunar material and its microwave penetration depth [J]. *Geochim. Cosmochim. Acta*, 2005, **69**(10): A805
- [18] Nishino M N, Maezawa K, Fujimoto M, et al. Pairwise energy gain-loss feature of solar wind protons in the near-

(continued on page 391)

pressurized modules, various space missions and experiments would be implemented. Astronauts would have a certain involvement in the scientific experiments. There might also be possible for them to be involved in implementing EVA construction/maintenance/replacement/expansion of the capacity of science facilities. The ability of transporting equipments and supplies to the station, retrieval of samples is expected. Also, complete coverage of telemetry/telecommand and information management in orbit will be implemented. China's space station is to run for about 10 years, so either the long term science experiments could be done, or with the support of Shenzhou or cargo spaceship, short term experiments would be also conducted.

Multidisciplinary researches in space science and exploration can be done in China's Space Station, which shows it is a great historical opportunities for the space science in this country.

## References

- [1] Chen Xiaodong, *et al.* From Dream to True [M]. Beijing: The PLA Literature and Art Publishing House, 2003. 1351
  - [2] Yang Liwei, Zuo Saichun. The First Taikonauts in the Space [M]. Beijing: People's Publishing House, 2003
  - [3] Gu Shuang. Understanding the Accompanying Small Satellite [M/OL]. People's Net, 2008, <http://scitech.people.com.cn/GB/132659/132689/132693/8121684.html>
  - [4] Gessa. CAS has completely fulfilled each experimental task for Shen Zhou No. 7 Space Ship [J]. *Bull. Chin. Acad. Sci.*, 2008, **23**(6):538-541
- 
- (continued from page 403)
- Moon wake [J]. *Geophys. Res. Lett.*, 2009, **36**, L12108, doi:10.1029/2009GL039049
  - [19] Sunshine J M, Farnham T L, Feaga L M, *et al.* Temporal and spatial variability of lunar hydration as observed by the deep impact spacecraft [J]. *Science*, 2009, **326**(5952):565-568
  - [20] Liu J J, Ren X, Mu L L, *et al.* Automatic DEM generation from CE-1's CCD stereo camera images [R]// 40th Lunar Planet. Sci. Conf. 2009 March 23-27, Woodlands, Texas, 2009. 2570
  - [21] Li Y Q, Liu J Z, Yue Z Y. NAO-1: A Lunar highland soil simulant developed in China [J]. *J. Aerosp. Engrg.*, 2009, **22**(1):53-57
  - [22] Zheng Y C, Wang S J, Ouyang Z Y, *et al.* CAS-1 lunar soil simulant [J]. *Adv. Space Res.*, 2009, **43**(3):448-454
  - [23] Jin Y Q, Fa W Z, Xu F. Modeling simulation and inversion for microwave active and passive remote sensing of the lunar surface [J]. *Remote Sensing Tech. Appl.*, 2007, **22**(02):129-134
  - [24] Li X Y, Wang S J, Chen F, *et al.* Methods and advances in research on lunar soil thickness [J]. *Acta Mineral. Sinica*, 2007, **27**(1):64-68
  - [25] Fa W Z, Jin Y Q. Inversion of lunar regolith layer thickness using microwave radiance simulation of three layer model and Clementine UV-VIS Data [J]. *Chin. J. Space Sci.*, 2007, **27**(1):55-65
  - [26] Fa W Z, Jin Y Q. Simulation of brightness temperature from lunar surface and inversion of regolith-layer thickness [J]. *J. Geophys. Res.: Planets*, 2007, **112**, doi:10.1029/2006JE002751
  - [27] Jiang J S, Wang Z Z, Li Y. Study on theory and application of CE-1 microwave sounding lunar surface [J]. *Eng. Sci.*, 2008, **10**(6):16-22
  - [28] Chan K L, Tsang K T, Kong B, Zheng Y C. Lunar regolith thermal behavior revealed by Chang'E-1 microwave brightness temperature data [J]. *Earth Planet Sci. Lett.*, 2010, **295**(6):287-291